JOURNAL OF MATERIALS SCIENCE 22 (1987) 4369–4376

Crystallization of the glassy phase in an Si_3N_4 material by post-sintering heat treatments

L. K. L. FALK, G. L. DUNLOP
Department of Physics, Chalmers University of Technology, S-412 96 Göteborg, Sweden

It is shown that post-sintering heat treatments in air in the temperature range 1100 to 1400° C result in substantial crystallization of the glassy phase in an Si_3N_4 material which was produced by the nitridation pressureless sintering (NPS) method using Y_2O_3 and Al_2O_3 as sintering aids. X-ray diffraction combined with analytical electron microscopy showed that the secondary crystalline phases which form are strongly dependent upon time and temperature of heat treatment as well as depth below the oxide scale. This effect is primarily due to the outward diffusion of cations (yttrium, aluminium and impurities) as well as the inward diffusion of oxygen. Small glassy pockets and thin amorphous intergranular films remain in the microstructure after heat treatment.

1. Introduction

Si_3N_4 materials, which are densified by a liquid-phase sintering process, contain a residual intergranular glassy phase inherited from the sintering medium [1]. This liquid forms above the relevant eutectic temperature through reaction between oxide sintering aids (such as Y_2O_3, Al_2O_3 or MgO), surface silica on the starting Si_3N_4 powder particles and some of the Si_3N_4 [2]. The oxynitride liquid, which is formed by this reaction, promotes densification by serving as a mass transport medium during sintering [1, 3, 4].

The presence of intergranular glass in Si_3N_4-based ceramic materials has a strong influence on their mechanical properties and oxidation behaviour [1, 5–7]. For example, softening of the intergranular glass phase at elevated temperatures, can promote grain-boundary sliding, cavitation creep and subcritical crack growth. Thus the onset of creep deformation and degradation of strength in these materials is strongly dependent upon the composition of the glassy phase [1]. It has, for example, been demonstrated that impurities such as calcium, which concentrate in the glassy phase, significantly impair the strength and creep performance of Si_3N_4 materials densified with MgO [8].

It has been shown that heat treatment of Si_3N_4 materials in an oxidizing environment after sintering can lead to improved strength [9–12], increased creep resistance [6] and increased resistance to oxidation [10]. It is thought that these improvements in properties arise from compositional changes in the material which affect the amount of intergranular glassy phase present in the microstructure. The glassy phase plays an important role in the elevated temperature oxidation behaviour because it provides a continuous transport medium between the interior of the material and its oxide scale. A reaction couple is formed between the intergranular glass and the SiO_2-rich oxide scale, enabling the outward diffusion of cations [13]. The intergranular regions also serve as a path for the inward diffusion of oxygen during oxidation [14]. These diffusion processes lead to an alteration of the composition of the intergranular amorphous phase, and such changes in composition affect the eventual formation of secondary crystalline phases from the intergranular glass.

Depending upon cooling rate and composition, secondary crystalline phases may form from the intergranular liquid in Si_3N_4 materials during cooling from the sintering temperature leaving only small amounts of residual intergranular glass in the microstructure [1, 15–17]. It has also been shown that the glassy phase in a β'-SiAlON material, with additions of Y_2O_3, can be crystallized to yttrium aluminium garnet, YAG, by a post-sintering heat treatment [18].

In the present work, microstructural changes which occur during the post-sintering heat treatment of a Si_3N_4 material containing Y_2O_3 and Al_2O_3, are investigated in some detail. The material, which was investigated, had been fabricated by the nitridation pressureless sintering (NPS) technique. This method involves the nitridation and subsequent pressureless sintering of compacts of submicrometre silicon and Si_3N_4 powders containing additions of sintering aids. The development of microstructure during fabrication of Si_3N_4 material by this method, using Y_2O_3 and Al_2O_3 as sintering aids, has been reported previously [19, 20]. The fully sintered material contains columnar grains of β-Si_3N_4 and a relatively large volume fraction of an oxynitride glassy phase containing yttrium, silicon and aluminium as well as impurities originating from the powder preparation. Preliminary work has shown that it is possible to partly crystallize this residual glass through heat treatment [21].

2. Experimental procedure

The experimental Si_3N_4 material was formed by the nitridation pressureless sintering (NPS) technique, which has been thoroughly described previously [22, 23]. The starting submicrometre powder compacts

0022–2461/87 $03.00 + .12

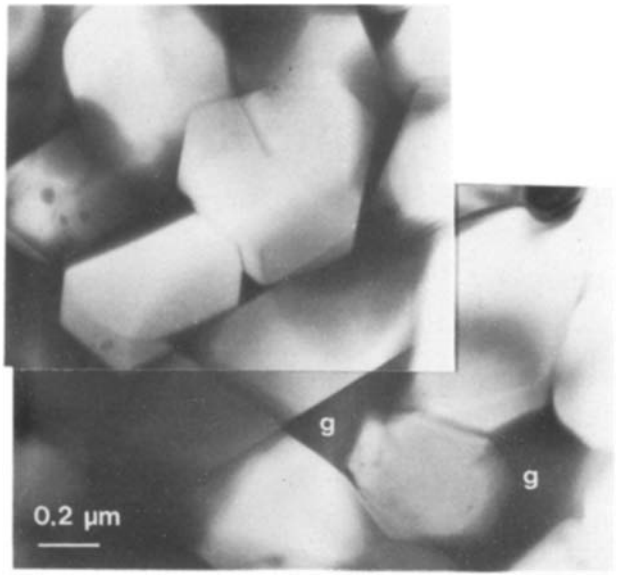

Figure 1 The general microstructure of the as-sintered NPS-Si_3N_4 material. The areas of dark contrast (g) are glass pockets containing substantial amounts of yttrium.

had a Si : Si_3N_4 mass ratio of 6 : 4 and were nitrided to 100% conversion of silicon to Si_3N_4 at 1350° C. The compacts contained additions of Y_2O_3 and Al_2O_3 such that a fully nitrided body contained the equivalent of 6 wt % Y_2O_3 and 2 wt % Al_2O_3. The nitrided compacts were embedded in an Si_3N_4 protective powder bed and pressureless sintered in a nitrogen atmosphere at 1850° C.

Heat treatments of fully sintered material were performed in air according to Table I. Both bulk samples in the form of cylinders with a diameter of 7 mm and a height of 3 mm and thin (60 to 80 μm) slices ready for ion-beam thinning to electron transparency were subjected to these heat treatments. The surfaces of the samples were polished with diamond paste (3 μm) prior to heat treatment.

TABLE I Temperatures and times used for heat treatment of the as-sintered material

Temperature (° C)	1100	1200	1300	1345	1400
Time (h)	6	0.15, 1, 6, 24	100	125	7

The microstructures of both the heat-treated and as-sintered materials were characterized using X-ray diffractometry and analytical transmission electron microscopy (TEM, STEM, EDX). Thin foils for TEM were prepared using standard techniques [20] and subsequently investigated in a Jeol 2000-FX TEM/STEM/SEM instrument with an attached Link 860 EDX system. Quantitative EDX analyses were performed using the Link RTS-2/FLS computer programme.

3. Results

3.1. As-sintered material

The microstructure of the as-sintered Si_3N_4 material consisted of β-Si_3N_4 grains surrounded by a glassy phase, Fig. 1. This amorphous phase was present as very thin, down to approximately 2 nm, intergranular films which merged into larger pockets at multi grain junctions, Fig. 2. Quantitative analysis of the glassy phase by STEM/EDX showed that the average elemental content (excluding light elements such as oxygen and nitrogen) was 25.5 wt % Si, 70.0 wt % Y and 4.5 wt % Al. It was found that the silicon and yttrium content varied by up to 10 wt % from the average between different pockets, while the aluminium content remained relatively constant. Small amounts of impurity elements such as calcium and iron were detected in some pockets. In order to avoid inaccuracies in analysis arising from spreading of the electron beam into adjacent β-Si_3N_4 grains, only the larger glass pockets were included in these analyses. No aluminium was detected in the β-Si_3N_4 grains indicating that the aluminium level was below the limit of

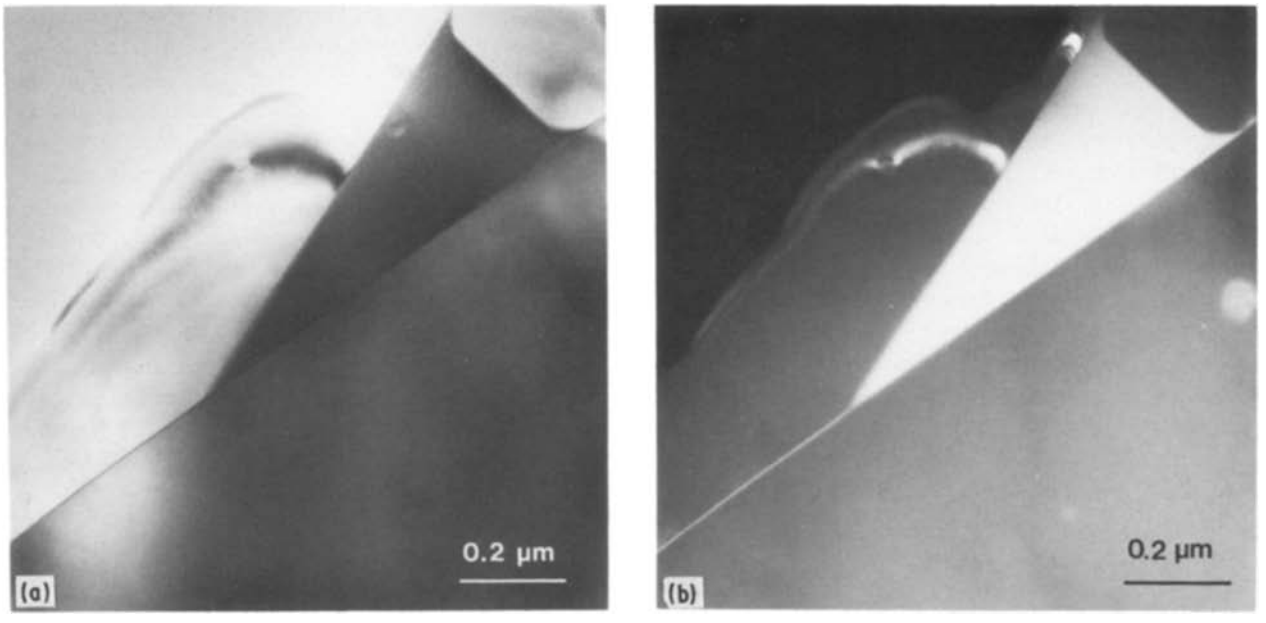

Figure 2 Thin amorphous film merging into a glass pocket at a triple grain junction in as-sintered material. (a) TEM bright-field. (b) Centred dark-field image taken using diffuse scattered electrons from the amorphous phase.

TABLE II Secondary crystalline phases identified by X-ray diffractometry in specimens heat treated at 1200° C for various times. α = α-$Y_2Si_2O_7$; W = Y,N-α-wollastonite ($YSiO_2N$); YS = Y_2SiO_5; A = Y,N-apatite

Time (h)	Secondary crystalline phases (in approximate order of predominance)
0.15	W, YS, A
1	
6	A, α, W, YS
24	

detectability, which under the experimental conditions used was expected to be ~2 wt %.

3.2. X-ray diffractometry of heat-treated material

X-ray diffractometry of bulk samples heat treated according to Table I showed that both time and temperature had a considerable effect on the resulting phase content of the material. Secondary crystalline phases formed during all of the heat treatments and examination by transmission electron microscopy (TEM) showed that only small amounts of glass remained in the microstructures.

In order to reveal microstructural gradients in the material under the oxide scale, the phases present in the bulk samples were determined by X-ray diffraction of polished sections at different depths below the oxidized surface. Depending upon temperature and time of heat treatment, as well as depth below the oxide scale, the following secondary crystalline phases were found to be present: yttrium silicate, Y_2SiO_5; yttrium disilicate, either α-$Y_2Si_2O_7$ or β-$Y_2Si_2O_7$; Y,N-α-wollastonite, $YSiO_2N$; Y,N-apatite, $Y_{10}(SiO_4)_6N_2$.

3.2.1. Effect of time on phases present after heat treatment at 1200° C

The secondary crystalline phases in specimens heat treated at 1200° C were determined for heat-treatment times of from 0.15 to 24 h. X-ray diffractograms were taken from sections at depths of 15 and 60 μm below the surface of the oxidized bulk samples but only after 24 h at 1200° C was any variation in phase content detected between these two depths. As shown in Table II, a significant change in the secondary crystalline phase content occurred between the times of 0.15 and 1 h. After the shorter heat-treatment time (that is 0.15 h) Y,N-α-wollastonite ($YSiO_2N$), yttrium silicate (Y_2SiO_5) and some Y,N-apatite had formed in the microstructure. Heat treatment for longer times (1 h and longer) resulted in a reduction of the wollastonite content, an increase in apatite content and the formation of a polymorph of yttrium disilicate (α-$Y_2Si_2O_7$). No significant changes in the phase content occurred after 1 h at the heat-treatment temperature of 1200° C with the exception that there was somewhat less Y,N-apatite close to the surface after 24 h.

3.2.2. Effect of temperature on secondary crystalline phases

X-ray diffractograms from the specimen heat treated 6 h at 1100° C gave virtually the same results as for 0.15 h at 1200° C; that is, a predominance of Y,N-α-wollastonite and Y_2SiO_5 with some Y,N-apatite.

Variations in the secondary phase content with depth below the oxidized surface were clearly detected in specimens subjected to heat treatment at 1300, 1345 and 1400° C. As shown in Table III, this was especially pronounced for the specimen which was heat treated at 1400° C for 7 h. No Y_2SiO_5 was found after heat treatment at temperatures between 1300 and 1400° C, but yttrium disilicate ($Y_2Si_2O_7$) was found to be present in these specimens. The particular polymorph of $Y_2Si_2O_7$ which formed was dependent both on temperature and depth below the surface. In material heat treated at 1300° C for 100 h both α-$Y_2Si_2O_7$ and Y,N-α-wollastonite were found in the near-surface region, while only β-$Y_2Si_2O_7$ could be detected just below the oxide scale in specimens heat treated at 1345 and 1400° C. The bulk of material heat treated at temperatures above 1300° C contained α-$Y_2Si_2O_7$, Y,N-α-wollastonite and Y,N-apatite.

3.3. Analytical transmission electron microscopy

Transmission electron microscopy (TEM) of heat-treated materials was carried out on specimens which had been heat treated in the form of thin (60 to 80 μm) slices. Crystallization had taken place in the larger glass pockets, Fig. 3, and there was a considerable variation in the morphology of the crystallized pockets for the different heat-treatment conditions. The secondary crystalline phases were always encompassed by residual glassy films.

3.3.1. Microstructures after heat treatment at 1100 and 1200° C

The microstructures of specimens heat treated at 1100° C for 6 h and at 1200° C for 0.15 h were virtually the same. All of the larger glass pockets had crystal-

TABLE III Secondary crystalline phases identified by X-ray diffractometry in material heat treated at higher temperatures. α = α-$Y_2Si_2O_7$; β = β-$Y_2Si_2O_7$; W = Y,N-α-wollastonite ($YSiO_2N$); A = Y,N-apatite.

Temperature and time	Depth below oxide scale					
	20–40 μm	100 μm	200 μm	250 μm	400 μm	1.5 mm
1300° C 100 h	α, W					α, W, A
1345° C 125 h	β			β, α, A		
1400° C 7 h	β	β	β, α, W, A		α, W, A	α, W, A

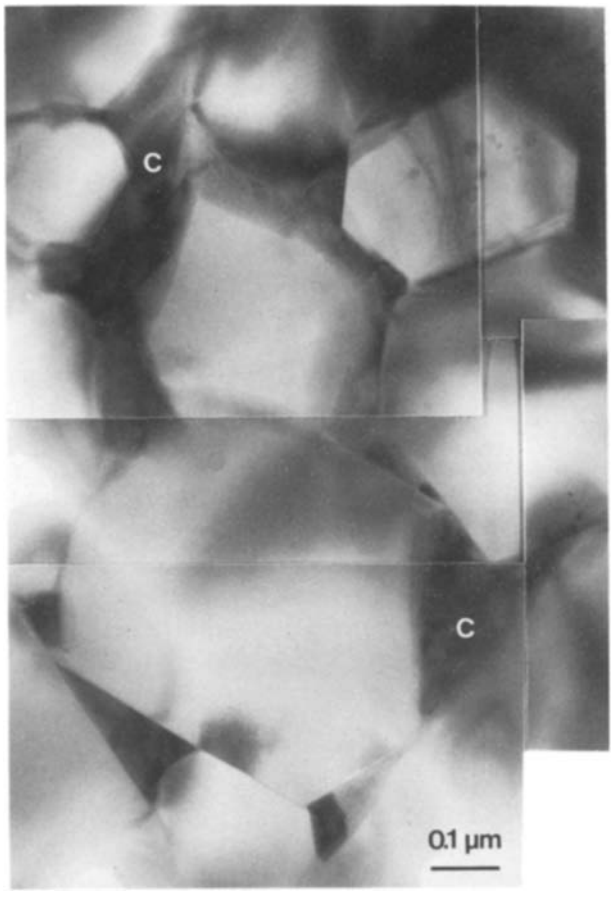

Figure 3 The microstructure of material after a post-sintering heat treatment of 0.15 h at 1200° C. All of the large intergranular pockets (e.g. C) have crystallized which gives rise to diffraction contrast in these areas.

lized, and most of them had a fairly complex structure. Usually several small grains had formed in the pockets, Figs 3 and 4, and, as shown by centred dark-field imaging using diffuse scattered electrons, these were separated by thin amorphous films. Microanalyses by STEM/EDX showed that the crystalline intergranular regions contained small amounts (2 to 5 wt %) of aluminium, indicating that some of the secondary phases identified by X-ray diffractometry contained dissolved aluminium.

After heat treatment for longer times at 1200° C (i.e. 1 h or more) no aluminium could be detected in the crystallized pockets, and these generally contained just one single grain as shown in Fig. 5. Dark-field imaging, Fig. 5b, clearly demonstrated the presence of a glassy film which separated the β-Si_3N_4 grains as well as separating the secondary crystalline phases from the surrounding β-Si_3N_4 grains. Lattice imaging, Fig. 6, also clearly showed the presence of an intergranular film in these regions. In this case the secondary phase was determined by selected-area electron diffraction to be the Y,N-apatite phase identified earlier by X-ray diffraction. The lattice fringes in the apatite grain in Fig. 6b correspond to an interplanar spacing of 0.41 nm while reflections from different sets of $\{1\,0\,\bar{1}\,0\}$ planes (d = 0.66 nm) were used for lattice fringe imaging of the adjacent β-Si_3N_4 grains.

Examination of a large number of intergranular pockets in material which had been heat treated for 24 h at 1200° C showed that only the larger pockets had crystallized. The observations are summarized in Fig. 7 where it can be seen that there was an apparent overlap between the partially crystallized pockets and pockets that had retained their amorphous structure. It should be born in mind that the measurements giving rise to Fig. 7 are from thin sections through glass pockets and therefore suffer from associated limitations of sampling. Nevertheless, it seems clear that there is a lower size limit for the glass pockets which crystallize during heat treatment.

3.3.2. Microstructures after heat treatment at 1300, 1345 and 1400° C

After heat treatment for 100 h or more at 1300 and 1345° C the microstructures were essentially similar to that obtained after 24 h at 1200° C. By way of contrast, however, heat treatment at 1400° C for 7 h resulted in the retention of glass in some fairly large pockets and these were determined by STEM/EDX to have a lower yttrium to silicon ratio than the glass phase in as-sintered material. The glass in these specimens had an internal structure consisting of spherical features, Fig. 8, which was also observed to a limited extent in material heat treated at 1345° C. Because these features did not exhibit diffraction contrast when the thin foils were tilted in the TEM, and also because

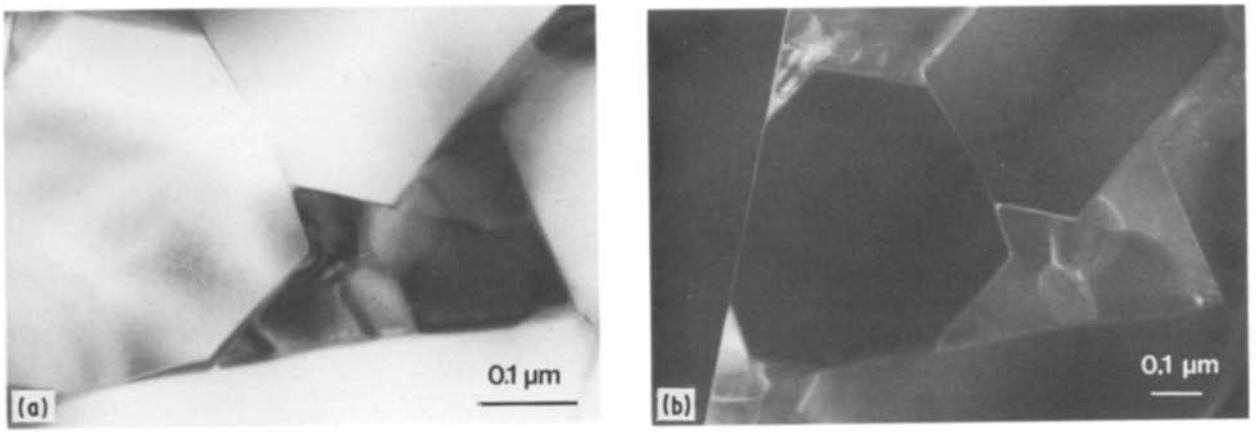

Figure 4 Pocket of fine secondary crystalline grains in material heat treated for 0.15 h at 1200° C. (a) TEM bright-field. (b) Dark-field using diffuse scattered electrons showing thin amorphous films which separate individual grains.

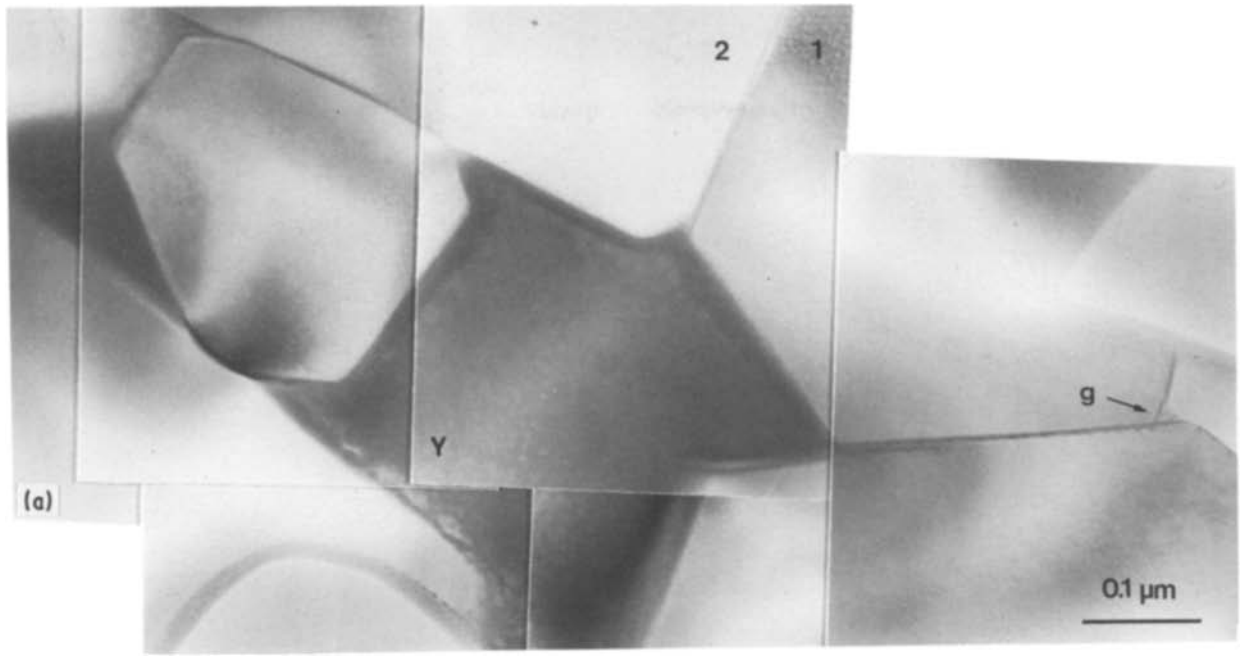

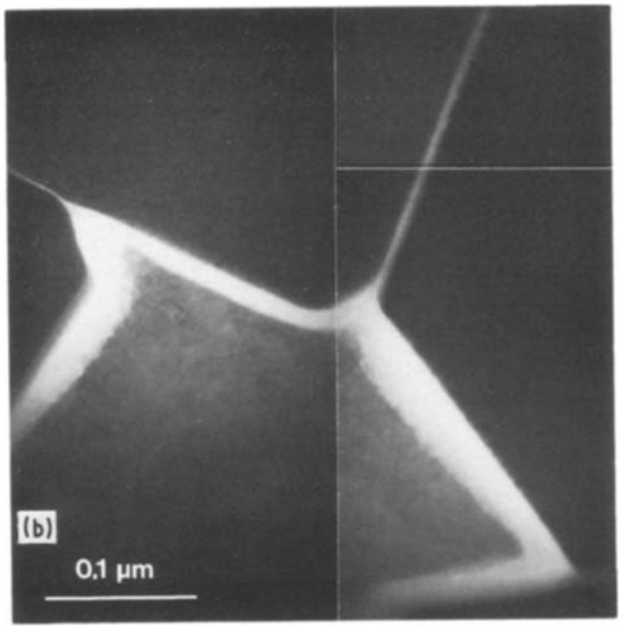

Figure 5 Region in the vicinity of a crystallized glass pocket in material heat treated 24 h at 1200° C. (a) TEM bright-field showing the crystallized pocket that contain Y,N-apatite (Y). Note also the small glass pocket (g) which did not devitrify during heat treatment. (b) Dark-field image showing the glassy film which surrounded the grains in this area.

they exhibited darker contrast than their surrounds in dark-field images using diffuse scattered electrons from an amorphous phase, it was surmised that they were either cavities or gas bubbles lying in the glass.

4. Discussion

It is evident that large-scale crystallization of the glassy phase in NPS-Si_3N_4 material can be affected by post-sintering heat treatments. As in the case of the SiAlON material which was investigated by Lewis *et al.* [18], the results show that a substantially crystalline material can be obtained.

The microstructure of heat-treated material is strongly dependent upon both temperature and time of heat treatment, and clearly these parameters should have a strong effect on the subsequent properties of the material. Even without special post-sintering heat treatments, Si_3N_4 materials which are used in elevated temperature service will also experience microstructural changes of the type shown here. Depending on the phases which crystallize this can have either a positive or negative effect on the properties of the material [1, 10, 24]. Some of the secondary crystalline phases that form in the Si_3N_4-SiO_2–Y_2O_3–YN pseudo ternary system are not stable in an oxidizing environment [24]. Their oxidation is associated with a molar volume change that introduces internal stresses that in turn could cause cracking of the material [1]. This is of considerable importance at temperatures below 1000° C, where oxidation of Si_3N_4 is negligible and therefore a protective surface layer of oxide does not form. The optimum composition of materials in this system is in the Si_3N_4–Si_2N_2O–$Y_2Si_2O_7$ compatibility triangle, which gives a polyphase material with good oxidation resistance and good mechanical properties [10, 24].

Substantial gradients in phase content were observed between the immediate sub-scalar region and the bulk of the material after heat treatment at 1300 to 1400° C. This was also observed to some extent after long times at 1200° C. These gradients in the secondary phase content reflect the previously observed elemental concentration gradients extending from the sub-scalar region to the bulk of the oxidized NPS-Si_3N_4 material [21]. The oxide scale was found to become rich in yttrium, aluminium and impurity elements such as calcium, potassium, titanium, vanadium and iron while a depletion of yttrium, iron and calcium was clearly detected in the sub-scalar region. The outward diffusion of cations is a direct consequence of the fact that the intergranular glassy phase is continuous throughout the material and also continuous with the amorphous part of the oxide scale. Concentration gradients for these elements exist between the interior

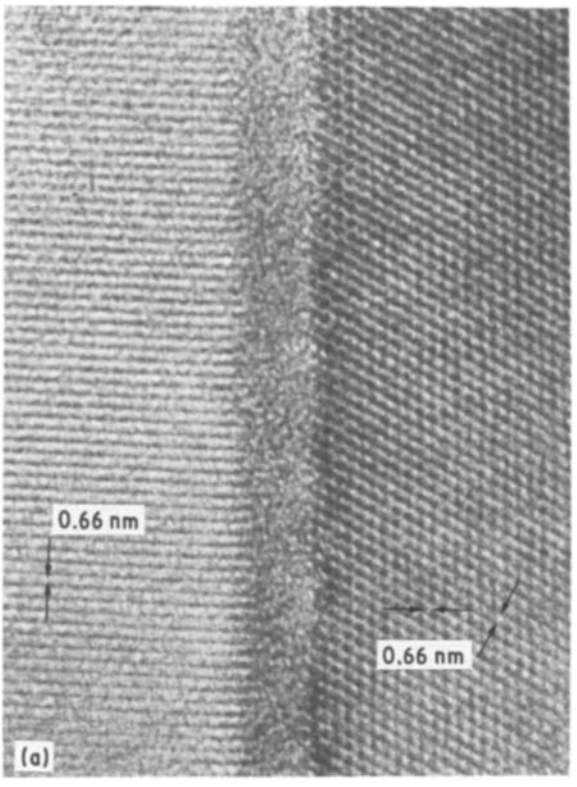

Figure 6 Lattice images showing the presence of intergranular films in the central region of Fig. 5. (a) Intergranular film between the β-grains 1 and 2 (see Fig. 5a). The lattice fringes correspond to $\{1\,0\,\bar{1}\,0\}$ planes (spacing 0.66 nm) in both grains. Grain 1 has an orientation which is close to an [0 0 0 1] beam direction giving rise to the two sets of lattice fringes visible in this grain. (b) Intergranular film in the vicinity of the triple junction between β-Si_3N_4 grains 1 and 2 and the Y,N-apatite grain. The lattice fringes in the Y,N-apatite grain correspond to the {2 0 0} planes with a spacing of 0.41 nm.

of the material and the oxide scale and therefore there is a strong driving force for their outward diffusion [13]. It has been suggested that this is an integral part of the mechanism of oxidation for polyphase Si_3N_4 materials [5, 13, 25].

As can be seen from Fig. 9, an outward diffusion of yttrium moves the composition of the sub-scalar material towards the Si_3N_4–SiO_2 side of the Si_3N_4–SiO_2–Y_2O_3–YN phase diagram resulting in the formation of phases, such as yttrium disilicate which contain less yttrium. Similar effects occur with respect to the oxygen/nitrogen content of the secondary crystalline phases in the sub-scalar region. It has been shown previously that, as well as the formation of an oxide scale, oxidation at high temperatures results in an increase in the amount of oxygen-containing phases within an Si_3N_4 material and it was concluded that the grain boundaries provided a favourable diffusion path for oxygen into the material [14]. The results presented in Table III lend support to these conclusions. Here it can be seen that the secondary crystalline phases which form close to the oxide scale, are phases which have a higher O : N ratio in their total anion content than those secondary phases which form in the interior of the material. In particular, only yttrium disilicate ($Y_2Si_2O_7$), which also has a lower yttrium content than the Y,N-apatite, forms in the region closest to the oxide scale at the higher temperatures of 1345 and 1400° C. The more yttrium-rich and nitrogen-containing Y,N-apatite phase is favoured at greater depths below the oxide scale.

In specimens heat treated at 1200 and 1300° C only the α polymorph of $Y_2Si_2O_7$ formed, but after heat treatment at 1345 and 1400° C there was a transition from the β to the α polymorph at a depth of around 200 μm below the oxide scale. Ito and Johnson [26] have reported a temperature of 1225 $\pm$ 10° C for the transition between the α and β polymorphs, α being the low-temperature form. The present work suggests, however, that the environment plays an important

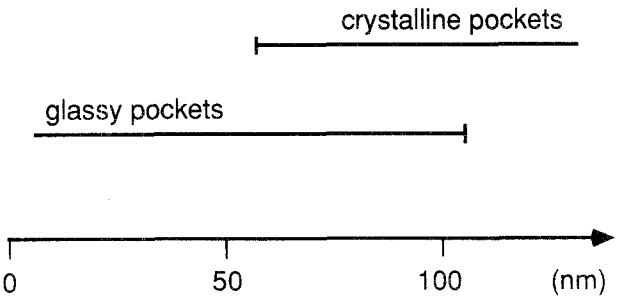

Figure 7 Sizes of crystalline and glassy pockets measured in thin foils from material heat treated at 1200° C for 24 h. The given sizes correspond to the diameter of the largest circle which could be placed within each pocket.

role in determining the particular polymorph which forms during crystallization. As discussed in the previous section, gradients in the elemental concentration of the intergranular regions build up during oxidation. The cation content of the region close to the scale decreases and the O:N ratio increases, which is especially pronounced in materials heat treated at 1350 and 1400° C.

Even under conditions, such as long-term heat treatments, which could be expected to favour large-scale crystallization of the glassy phase it was found that a residual thin film of glassy phase was retained at all grain boundaries and that the smallest glass pockets remained uncrystallized. This was clearly shown by dark-field imaging of the amorphous phase and also by lattice fringe imaging of adjacent grains (see, for example, Figs 5 and 6). The fact that smaller pockets did not crystallize at all is in agreement with the predictions of Raj and Lange [27, 28]. If it is assumed that the composition of these small glassy regions in as-sintered material is similar to that of the larger pockets that did crystallize, then a major obstacle to their crystallization still arises because of mechanical constraints from the surrounding crystalline material. The volume change associated with crystallization introduces a strain energy which opposes the transformation. Raj and Lange's theory predicts that a glass pocket in a polyphase material must have a certain volume before crystallization can take place [27, 28].

The fine grain size of the crystallization products which were obtained after short-term heat treatment at 1200° C, and also after 6 h at 1100° C, indicate that a number of crystal nuclei form in each large glass pocket in the early stages of heat treatment at these temperatures. Growth from these nuclei gave fine-grained structures which subsequently coarsened. After just 0.15 h at 1200° C these newly crystallized areas contained significant amounts of aluminium, but after 1 h or more aluminium could not be detected in the new secondary grains. This indicates that aluminium had either diffused in to the β-Si_3N_4 grains, together with oxygen, to form a dilute β'-SiAlON solid solution, or that it diffused via the residual glass phase to the surface oxide as has been observed at higher temperatures [21].

The relatively large volumes of glassy phase retained in specimens which were heat treated at 1400° C could be a result of the presence of a liquid phase during heat treatment at this high temperature. Microanalyses by STEM/EDX showed that the fairly large glass pockets had a considerably lower Y:Si ratio than the glass pockets in as-sintered material. This is consistent with a substantial decrease of the cation content of the intergranular glassy phase during high-temperature oxidation. The lowest reported eutectic temperature in the SiO_2–Y_2O_3–Al_2O_3 system is at ~ 1345° C [29] for SiO_2-rich compositions, but more recent measurements indicate that this eutectic is at ~ 1380° C [30]. This supports the suggestion that a liquid phase is present in this material during heat treatment at 1400° C. The large spherical cavities which were observed in the glassy pockets after heat treatment at 1345 and 1400° C could be an indication of a formation of gas bubbles in the liquid. These bubbles could contain either N_2 or SiO arising from oxidation of Si_3N_4 or the secondary crystalline phases, or decomposition of the liquid phase.

5. Conclusions

1. The glassy phase in an Si_3N_4 material fabricated

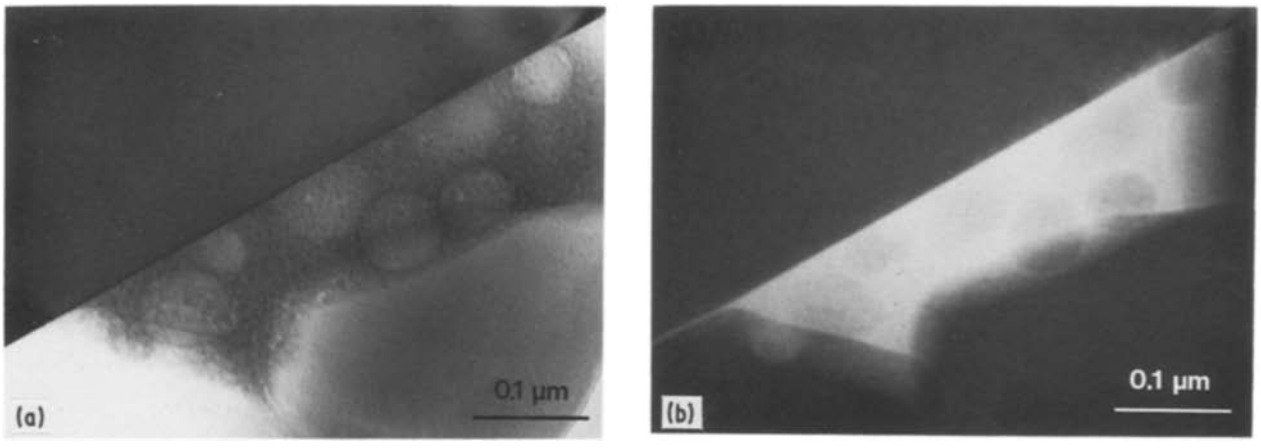

Figure 8 Intergranular pocket containing a glassy phase after heat treatment for 7 h at 1400° C. The spherical features are probably cavities or gas bubbles. (a) TEM bright-field. (b) Dark-field from diffuse scattered electrons. Note that the spherical features have darker contrast than their surrounds.

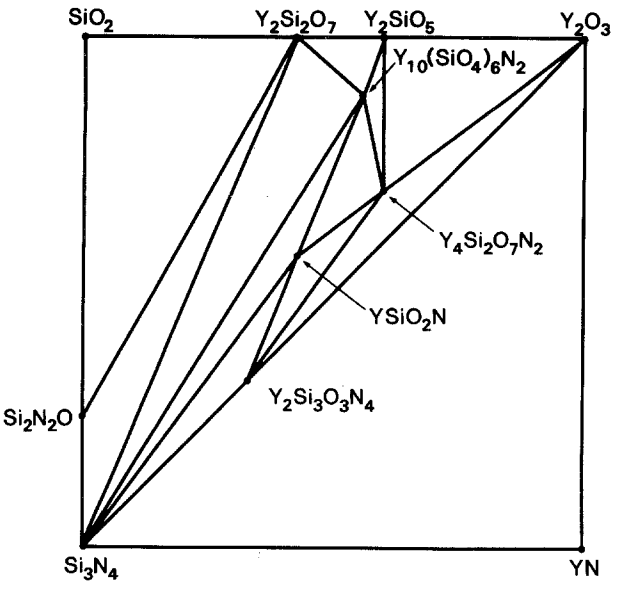

Figure 9 Phase relations in the system Si_3N_4–SiO_2–Y_2O_3–YN. After data presented in [31].

by the nitridation pressureless sintering (NPS) method using Y_2O_3 and Al_2O_3 as sintering aids can be substantially crystallized by post-sintering heat treatments in air at temperatures in the range 1100 to 1400° C.

2. Crystallization takes place in the larger glass pockets while smaller glass pockets and intergranular films remain undevitrified.

3. After heat treatment, all of the grains in the material were surrounded by films of a residual glassy phase.

4. Because of phase transformations and compositional changes which occur in the intergranular regions during heat treatment, the type of secondary crystalline phases in the material is strongly dependent upon time and temperature of heat treatment as well as depth below the oxide scale.

5. The variation of secondary crystalline phases with depth below the oxide scale is due to the outward diffusion of cations (yttrium, aluminium, impurities) to the scale as well as the inward diffusion of oxygen.

6. A considerable amount of liquid phase is present in the material during heat treatment at 1400° C. This results in a large volume fraction of residual glassy phase after heat treatment.

Acknowledgements

The experimental material was kindly supplied by R. Pompe of the Swedish Institute for Silicate Research with whom stimulating discussions were held. Financial support from the Swedish Board for Technical Development is gratefully acknowledged.

References

1. F. F. LANGE, *Int. Met. Rev.* **1** (1980) 1.
2. F. F. LANGE, in "Nitrogen Ceramics", edited by F. L. Riley (Noordhoff, Leyden, 1977) pp. 491–509.
3. M. H. LEWIS and R. J. LUMBY, *Powder Met.* **26** (1983) 73.
4. S. HAMPSHIRE and K. H. JACK, in "Special Ceramics, 7", edited by D. Taylor and P. Popper (British Ceramic Research Association, Stoke-on-Trent, 1981) pp. 37–49.
5. M. H. LEWIS and P. BARNARD, *J. Mater. Sci.* **15** (1980) 443.
6. B. S. B. KARUNARATNE and M. H. LEWIS, *ibid.* **15** (1980) 449.
7. C. O'MEARA, P. H. M. NILSSON and G. L. DUNLOP, *Metals Forum* **8** (1985) 194.
8. J. L. ISKOE, F. F. LANGE and E. S. DIAZ, *J. Mater. Sci.* **11** (1976) 908.
9. F. F. LANGE, B. I. DAVIS and M. G. METCALF, *ibid.* **18** (1983) 1497.
10. F. F. LANGE, B. I. DAVIS and H. C. GRAHAM, *J. Amer. Ceram. Soc.* **66** (1983) C-98.
11. D. R. CLARKE, F. F. LANGE and G. D. SCHNITTGRUND, *ibid.* **65** (1982) C-51.
12. A. TSUGE, K. NISHIDA and M. KOMATSU, *ibid.* **58** (1975) 323.
13. D. R. CLARKE and F. F. LANGE, *ibid.* **63** (1980) 586.
14. W. J. McDONOUGH, C. Cm. WU and P. E. D. MORGAN, *ibid.* **64** (1981) C-45.
15. D. R. CLARKE and G. THOMAS, *ibid.* **61** (1978) 114.
16. *Idem, ibid.* **60** (1977) 491.
17. O. I. KRIVANEK, T. M. SHAW and G. THOMAS, *ibid.* **62** (1979) 585.
18. M. H. LEWIS, A. R. BHATTI, R. J. LUMBY and B. NORTH, *J. Mater. Sci.* **15** (1980) 103.
19. L. K. L. FALK, R. POMPE and G. L. DUNLOP, in "Science of Ceramics 12", edited by P. Vincenzini (Ceramurgica s.r.l., Faenza, 1984) pp. 293–8.
20. L. K. L. FALK, R. POMPE and G. L. DUNLOP, *J. Mater. Sci.* **20** (1985) 3545.
21. L. K. L. FALK, G. L. DUNLOP and R. POMPE, *Mater. Sci. Engng* **71** (1985) 123.
22. R. POMPE, L. HERMANSSON and R. CARLSSON, in "Engineering with Ceramics", edited by R. W. Davidge (British Ceramic Society, Stoke-on-Trent, 1982) pp. 65–74.
23. R. POMPE, L. HERMANSSON and R. CARLSSON, *Sprechsaal* **115** (1982) 1098.
24. F. F. LANGE, S. C. SINGHAL and R. C. KUZNICKI, *J. Amer. Ceram. Soc.* **60** (1977) 249.
25. S. C. SINGHAL, *J. Mater. Sci.* **11** (1976) 500.
26. J. ITO and H. JOHNSON, *Am. Mineral.* **53** (1968) 1940.
27. R. RAJ and F. F. LANGE, *Acta Metall.* **29** (1981) 1993.
28. R. RAJ, *J. Amer. Ceram. Soc.* **64** (1981) 245.
29. I. A. BONDAR and F. J. GALAKOV, *Izv. Akad. Nauk SSSR, Ser. Khim.* **7** (1964) 1325.
30. C. O'MEARA, G. L. DUNLOP and R. POMPE, in "High Tech Ceramics" edited by P. Vincenzini, Materials Science Monographs, 38A (Elsevier, Amsterdam, 1987) pp. 265–270.
31. L. J. GAUKLER, H. HONKE and T. Y. TIEN, *J. Amer. Ceram. Soc.* **63** (1980) 35.

Received 26 January
and accepted 15 April 1987